ORDER IN LANGMUR-BLODGETT FILMS OF LEAD AND CADMIUM STEARATE: AN X-RAY DIFFRACTION STUDY

A. Malik,* M.K. Durbin, A.G.Richter,* K.G. Huang† and P. Dutta*

*Department of Physics and Astromony, Northwestern University, Evanston, IL 60208 USA

†Materials Science Division, Argonne National Laboratory
Argonne, IL 60439 USA

Materials Science Division
Argonne National Laboratory
Argonne, IL 60439

August 1995

/jc

Distribution:

1-2. M. J. Masek
3. B. D. Dunlap
4. P. A. Montano
5. F. Y. Fradin
6. R. Gottschall
7. Editorial Office
8. Authors

Submitted to Physica B.

This work is supported by the Division of Materials Sciences, Office of Basic Energy Sciences of DOE, under contract No. W-31-109-ENG-38.

Last update: 6/25/95, 10:35:14 AM -- preprint, accepted for publication in NIM-A --

Concentration of Synchrotron Beams by Means of Monolithic Polycapillary X-Ray Optics

J.B. Ullrich[a,b], K.G. Huang[c], S.M. Owens[a], D.C. Aloisi[a], F.A. Hofmann[a], N. Gao[a], I.L. Klotzko[a,b], W.M. Gibson[a]

[a] *Center for X-Ray Optics, University at Albany, SUNY, Albany, NY 12222, USA*

[b] *X-Ray Optical Systems Inc., 90 Fuller Rd., Albany, NY 12205, USA*

[c] *Materials Science Division, Argonne National Laboratory, Argonne, IL 60439, USA*

Capillary Optics have proven to be a valuable tool for concentrating synchrotron radiation [1]. Single tapered capillaries are used at several facilities. However, most of these optics collect only over a small area. This can be overcome by using larger capillary structures. Polycapillary optics can deflect x-rays by larger angles than other x-ray optics that use only one or two reflections. Conventional x-ray optics that achieve similar deflections, are much more energy selective than capillaries. Therefore, capillaries achieve very short focal distances for a wide range of energies. The measurements shown here represent first tests performed with polycapillaries of large input diameter. The performance with respect to transmission efficiency and spot size was evaluated for a set of four very different prototypes. It is shown that a significant gain may be achieved if a spot size of the order of 0.1 mm is required. Further, some characteristics of the different optics are discussed.

1. Introduction

X-Rays can be deflected by total external reflection [2]. Capillaries allow to use multiple reflections to guide x-rays over larger angles. Losses due to absorption can be kept small even if the capillary is being bend over several degrees [3]. Assemblies of such capillaries can be used to collimate x-rays from a point source as well as concentrating x-rays from a parallel beam like a synchrotron. Compact design and good performance over a wide energy band are major advantages of these optics versus conventional x-rays optics. For these measurements, monolithic polycapillary x-ray optics where used. Instead of using an array of fibers and aligning them by a grid, the fibers where fused together to a one piece optic. This allows for a more compact design and relaxes the restrains for careful handling. A sketch of such an optic is shown in Fig. 1.

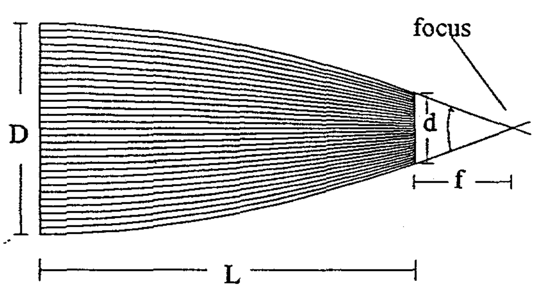

Fig. 1: Sketch of a monolithic capillary optic.

Each channel is individually tapered as the lens itself is tapered. The channels are close packed all the way through the lens.

2. Measurements

2.1 Setup

The beamline used, X6B at the National Synchrotron Light Source at Brookhaven National Lab., includes a monochromator as well as a focusing mirror. For the experiments discussed here, the focusing was not desirable. Therefore the mirrors where adjusted in such a way that the beam width was comparable to the width of the lens input (*D*). The height of the beam was much smaller than that. It was about

0.5 mm. The beam first passed through a transmission ion chamber. After that it hit the lens which was held by a motion controlled stage to allow alignment with the beam. The beam then hit another ion chamber. It was possible to bring a lead knife edge between the output of the lens and the second ion chamber. It was mounted on a precision stage to allow scans of the focal spot. In front of the lens a four slit collimator allowed to adjust the beams size for localized measurements. The setup is sketched in Fig. 2.

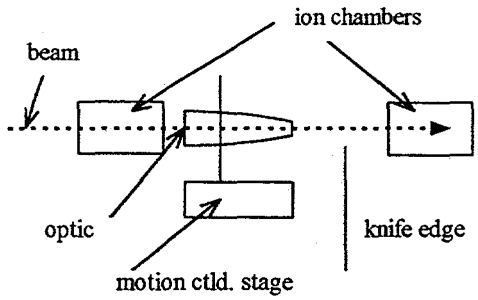

Fig. 2: Sketch of the setup.

It was easily possible to move the lens out of the beam in order to normalize the two ion chambers.

2.2 Geometry

The lenses used were picked to cover a wide range of possible geometries. The properties are summarized in Table 1.

Lens	15.15	I945	I9483A	5.5.2
D (mm)	6.95	8.0	4.5	7.0
d (mm)	0.5	5.5	3.5	2.0
L (mm)	154	24	70	120
C (µm)	47.5	19	14	88
c (µm)	2.5	12	10	20

Table 1: Geometry of the lenses.

Lens 15.15. has the smallest output end and the smallest focal spot was expected for this lens. On the other hand, the small end is almost closed up and the shape of the lens is very irregular. Lens I948 is almost not tapered. A large focal spot and a high transmission efficiency is expected for this lens. The details of the profile will be discusses later.

2.3 Transmission Efficiency

One of the most important performance numbers for a capillary optics is the transmission efficiency. It is given by the ratio of photons leaving the lens over the number of photons entering it.

The used beam exposed only a small line across the lens. Due to this, a higher fraction of straight channels in the center was exposed. If all of the lens would have been exposed by the beam, the transmission efficiency would have been significantly lower. It is not possible to estimate the total transmission efficiency correctly using the data obtained. To estimate the total transmission efficiency, it is necessary to account for local variations of the transmission efficiency. These local variations have different sources. Firstly, with increasing distance from the center, the deflection increases. The transmission decreases therefore. How fast the transmission decreases depends largely on the exact shape of the taper. Secondly, some lenses show closed sections that do not transmit at all. These section can be found using a point source. The point source is placed in the focal spot and a film is exposed at the parallel end. To obtain a more quantitative result, a pinhole and a detector may be used instead. In the experiment discussed here, the lens was scanned through the beam to obtain a measure for the uniformity. These measurements will be discussed later.

The used lenses showed a wide range of transmission efficiencies. This corresponds to the wide range of geometries. The lowest transmission efficiency was measured for lens 15.15. Lens 15.15 was tapered down to a very small tip. Both ends showed a very low open area. At the input end, the wall thickness was about half the capillary diameter. At the output, the walls where about twice as thick as the channels wide. The channels where not hexagonal but round. The overall shape of the lens showed clearly visible, multiple inflection points. All these factors reduce the transmission efficiency a lot. The measured efficiency was less than 0.1 %.

Lens	15.15	I945	I9483A	5.5.2
τ (%)	< 0.1 %	15 %	45 %	< 1%
f (mm)	6	28	110	15
s_{theo} (mm)	0.03	0.12	0.45	0.08
s (mm)	0.05	0.12	0.37	0.21

Table 2: Transmission (τ) at 8 keV, focal distance (f) and spot size (s).

On the other hand, lens I9483A transmitted 45 % of the photons. This lens is almost straight. The taper ratio, obtained by dividing input and output diameter, is only about 5/4, while the taper ratio is about 14 for lens 15.15.. The transmission efficiency is tabulated in Table 2.

The transmission efficiencies given here, also carry some error since the normalization of the detectors does not take the spatial non-uniformities of the detectors into account. In the case with lens, a different part of the second detector is exposed as in the case without lens.

2.4 Spot Size

To estimate the spot size for an ideal lens, two factors have to be taken into account. The channel size is a lower limit for the expected source size. Additionally, due to the divergence of the x-rays leaving each channel, the spot size is limited by this divergence and the distance of the focal spot.

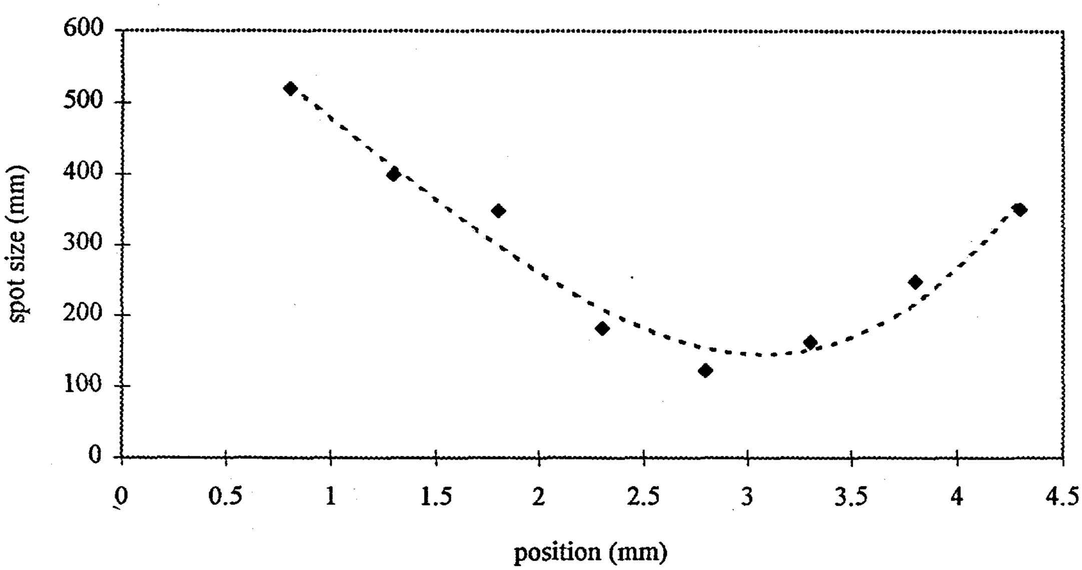

Fig. 3: Spot size as a function of the distance from the output of lens I945A.

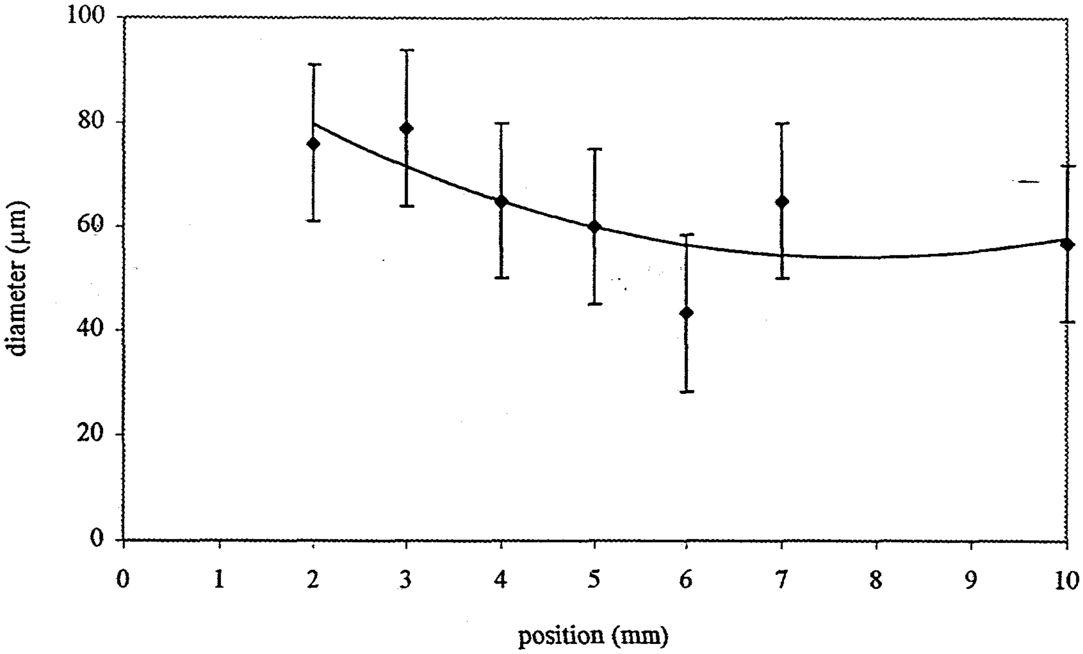

Fig. 4: Spot size for different distances from the output of lens 15.15. .

Since the output divergence (2θ) for each channel is about the same as the critical angle (θ_c), the spot size can be approximated by:

$$s = c + f\tan(\theta_c). \quad (1)$$

where s is the spot diameter, c the diameter of the channel at the output, and f the focal distance. For a real lens, the spot size may be enlarged due to misaligned channels or due to irregular channel diameters. The measured spot size for lens I9545A fits nicely this theoretical calculation. The measured spot size for lens I9483 is smaller than expected. Since this lens is almost not tapered, the x-rays are involved in very few reflections. For this case, the output divergence depends on the input divergence, since it is smaller than the critical angle. Therefore, the assumption that the output divergence is close to the critical angle is not valid anymore. If a smaller output divergence of 3 mrad, instead of 4 mrad, is assumed, the measured spot size fits the calculation.

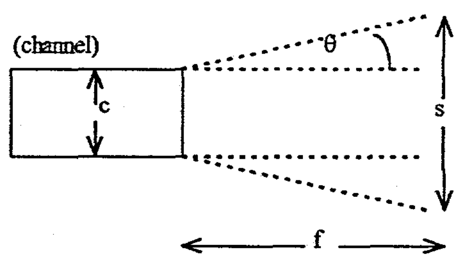

Fig. 5: Sketch of parameters needed to calculate the focal spot size.

The spot size, as well as the focal distance, is also tabulated in Table 2. It was measured using a lead knife edge. The knife edge was mounted on a precision translation stage. It was scanned horizontally through the beam. This scans where done at different distances from the output of the lens to find the focal spot. The resolution of the knife edge was about 10 µm. Lens 15.15 shows the smallest spot size. But this is less due to concentration but more due to the fact that only the center capillaries transmit. The beam size does vary only little for different distances. A plot for lens 15.15 is shown in Fig.

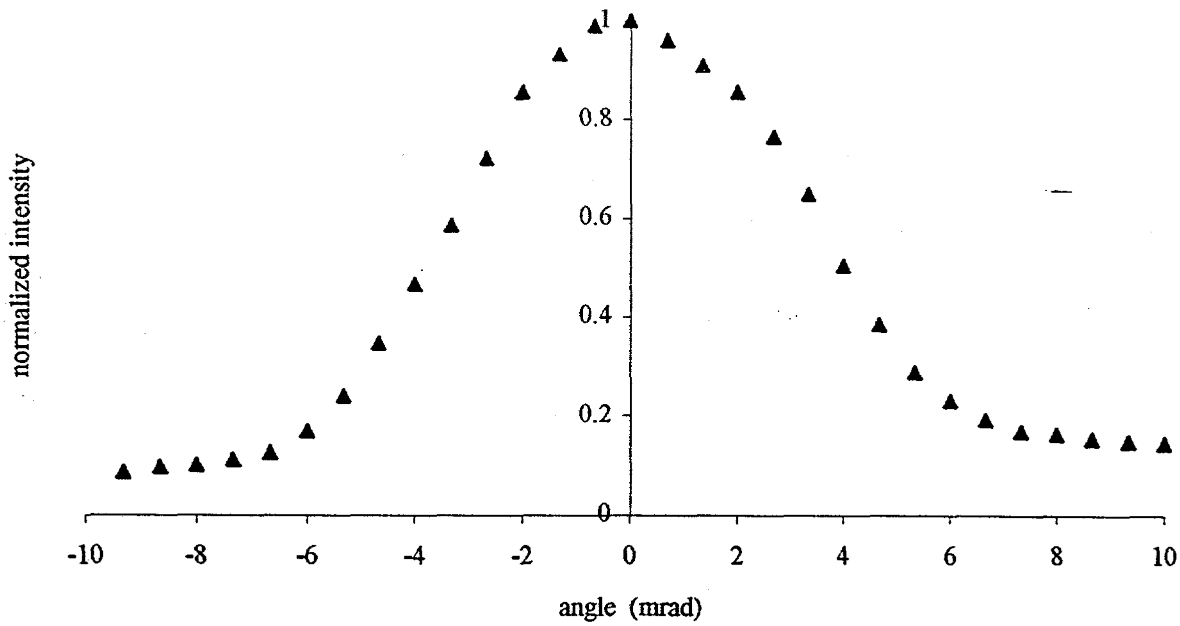

Fig. 7: Tilt scan of lens 5.5.2.

4. This measurement was also hindered by the low transmission.

Fig. 3 shows the same measurement for the well performing lens I945A.

2.5 *Angular Acceptance*

The angular acceptance of the lens was

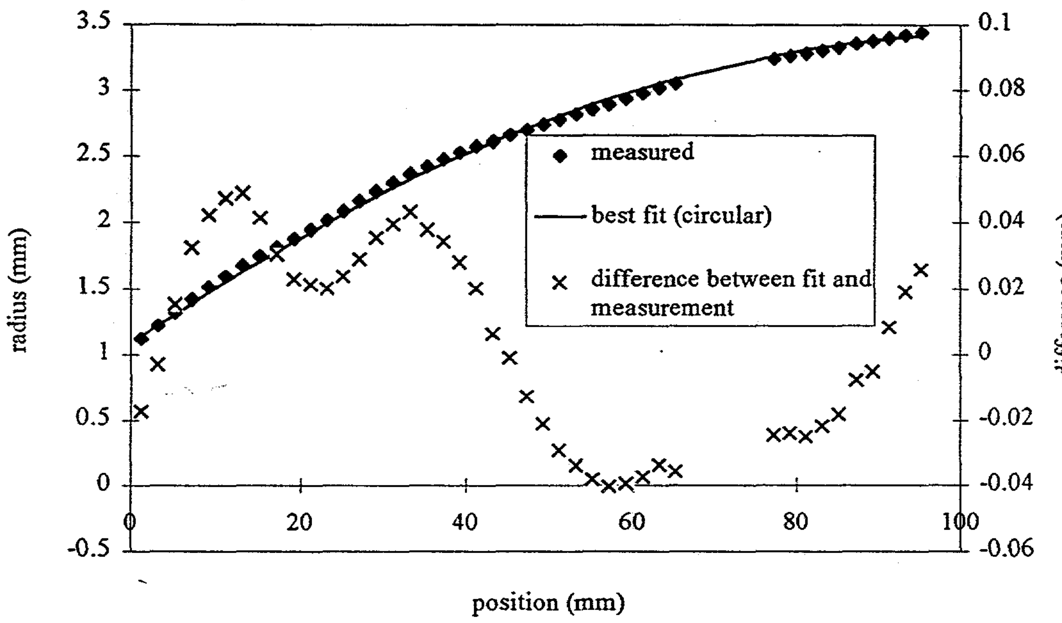

Fig. 6: measured profile of lens 5.5.2 and best fit. The gap in the measured data is due to a label that was attached to the lens.

measured by tilting and turning the lens in the beam. It is important to know about the angular acceptance to check if the input of the lens is parallel. This backs up point source measurements. If a point source is placed in the focal spot of the lens, the alignment of the channels at the parallel end can be checked by scanning the rocking curve of a crystal.

Since one of the strong points of this optics is its use in existing beamlines, it is also important to know what kind of divergence the optic is able to accept, since an existing beamline may have a unique divergence characteristics due to already build in optical devices. The accepted divergence has to be taken into account when the usefulness of the optic is evaluated.

For a well build optic, where all the channels are aligned parallel to each other at the input, the input acceptance is given by the critical angle.

However, the analysis of the measurements done at X6B is somewhat more difficult due to the convergence of the beam.

Due to the way the lens was mounted, the input moved whenever the lens was tilted or rotated.

The raw data, without any of these corrections applied, shows an angular acceptance of a few mrad. An example is shown in Fig. 7.

2.6 Uniformity

Like mentioned earlier, only a small part of the lens was exposed to the beam. To get a better estimate of the overall performance of the lens, the lens was scanned vertically through the beam.

For lens I945A the beam size was limited to 0.4x0.4 mm. The lens was scanned horizontally and vertically through the beam. The result of this scan is shown in Fig. 8.

If a point source is placed in the focus of a lens and a piece of film close to the parallel end of the lens, high resolution x-ray micrographs can be obtained. They show qualitative non-uniformities and closed channels [4].

2.7 Profile

To understand the low transmission efficiency of some of the lenses better, the

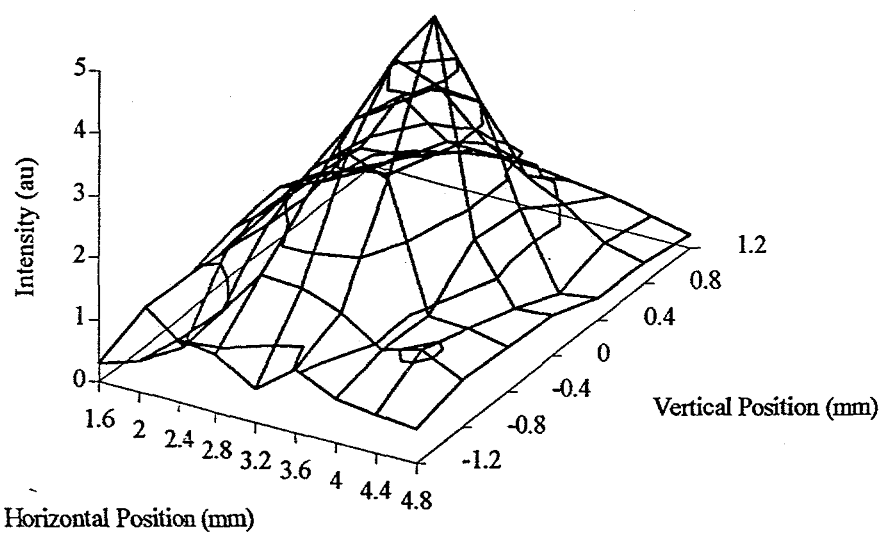

Fig. 8: Intensity at the output of lens I945A for different beam positions.

profile was measured. To do this with the required precision, a microscope based system was used. It allowed to determine the radius as a function of position with an error of less than 10 μm. Some of the lenses where evaluated that way earlier. Lens I945 is not at all circular bend. Its profile fits a gausian curve very close [5]. If this profile is used to predict the transmission efficiency, the prediction fits very close the measurement for a point source.

The profile of lens 5.5.2 fits very closely a circular profile. But upon closer investigation, some deviation can be found. This deviation is of the same magnitude as the channel diameter. It may therefore effect the transmission significantly. This profile is shown in Fig. 6. The lens was also bend overall by about the same amount.

2.8 Radiation Damage

Since it was not desirable to sacrifice any of the samples for radiation damage experiments, only some preliminary studies were undertaken. Each lens showed darkening as soon as it was exposed. It became clearly visible after only a few seconds. There is no data available during this time since it took some time to align the optic in the beam. One optic, I948A, was exposed for a longer time after it was aligned. After being exposed for 5 hours at 8 keV, the transmission decreased from 45 % to 38 %. The part that was hit by the beam was dark black by than. The beam footprint was visible at both ends of the lens. This suggests radiation damage all the way through the lens. Further studies have to be undertaken. Measurements with single capillaries do not show the same dark color even at much higher dose in a white beam. On the other hand, these capillary measurements show that it may be possible to reverse some of the damage by annealing.

2.9 Gain

Any figure of merit derived from these measurement has to be used with care. Firstly, the beam used was not the beam that promises the best gain for a focusing optics. Secondly, each possible application has to be evaluated separately since each one allows for special optimizations. As a general gain number, the flux in the focal spot over the flux density at the input of the beam will be used. To take the special circumstances of this experiment into account, two different gains where calculated. The first gain takes only a concentration in one dimension into account. This corresponds the situation found at the experiments described earlier. For a beam that exposes the full lens, concentration takes place in two dimensions. To calculate the appropriate gain, the transmission was corrected. To do so, earlier point source measurements where used. The result is shown in Table 3.

Lens	15.15.	I945	I9483A	5.5.2.
G_{1D}	0.07	10	6.1	0.17
G_{2D}	0.97	135	45	1.1

Table 3: Gain for a concentration in one dimension (G_{1D}) and in two dimensions (G_{2D})

3. Conclusion

The measurements shown here support earlier estimates of the performance of larger monolithic polycapillary optics. As mentioned earlier in this paper, it should be stressed that these optics have very unique properties that may be applicable to a wide range of application. Neither throughput nor spot size are as exceptional as for mirrors or coherent optics like Bragg-Fresnel zone plates. On the other hand, the optics discussed here prove to be very easily included in existing systems. They provide an opportunity to easily upgrade beamlines without making permanent changes to the beamline. The inherent broadband character makes it easy to include the optics whenever energy scans over a larger energy band are required. The short focal distance relaxes the space constraint usually found at synchrotron beamlines. Further developments will largely depend on better profile control. Measures to achieve this are under way.

Acknowledgments

The authors wish to acknowledge support under NASA contract NAS8-39926.

References

[1] D.J. Thiel, E.A. Stern, D.H. Bilderback, A. Lewis, Physica B 158 (1989) 314.
[2] A.H. Compton, Phil. Mag 45 (1923) 1121.
[3] J.B. Ullrich, V. Kovantzev and C.A. MacDonald, J. Appl. Phys. 74 (1993) 5933.
[4] J.B. Ullrich, W.M. Gibson, M.V. Gubarev, C.A. MacDonald, Qi-Fan Xiao, Nucl. Inst. & Meth. A 347 (1994) 401.
[5] SPIE